Cell Tissue Res (1988) 251:555–564

Cell and Tissue Research
© Springer-Verlag 1988

Structure of the cumulus matrix and zona pellucida in the golden hamster: A new view of sperm interaction with oocyte-associated extracellular matrices

Ashley I. Yudin[1], **Gary N. Cherr**[2], **and David F. Katz**[1]

[1] Department of Obstetrics and Gynecology, School of Medicine, University of California, Davis, California, USA;
[2] Bodega Marine Laboratory, University of California, Bodega Bay, California, USA

Summary. Hamster oocyte-cumulus complexes (OCC), with and without sperm, were structurally analyzed by light- and electron microscopy using freeze substitution. This method has yielded a clear picture of the extracellular oocyte investments, the cumulus cell matrix and the zona pellucida. The cumulus matrix has an overall homogeneous fibrillar structure which appears to attach to cumulus cells at their filopodial extensions. The matrix also extends into the outer regions of the zona pellucida. The zona pellucida has a distinct porous configuration throughout its entire structure. During gamete interaction experiments, capacitated hamster sperm with ultrastructurally intact acrosomes were found throughout the matrix. Sperm had dramatic effects on the matrix, resulting in compression and stretching. Sperm found on the zona pellucida had initiated or completed the acrosome reaction. During the initial stages of the acrosome reaction, the matrix was in contact with the sperm. At later stages of the acrosome reaction, there was a complete loss of matrix material in regions near the sperm.

Key words: Cumulus – Zona pellucida – Extracellular matrix – Sperm – Fertilization – Golden hamster

Immediately prior to fertilization, mammalian sperm must traverse two extracellular egg investments, the cumulus matrix and the zona pellucida. The former is a viscoelastic extracellular matrix consisting of glycosaminoglycans, primarily hyaluronic acid (Ball et al. 1982), while the latter is a highly structured investment containing 3–5 glycoproteins (see Dunbar and Wolgemuth 1984, for review). Mechanisms of sperm penetration of the cumulus and zona remain incompletely understood and are, to some extent, controversial (Talbot 1985). The principal active processes are mechanical forces generated by the motile flagellum and digestion of the extracellular egg investments by sperm enzymes. The latter may be intimately linked to the time course of the sperm acrosome reaction.

It is not clear whether hyaluronidase in the sperm acrosome and/or on the sperm surface is involved in sperm passage through the cumulus matrix (Zao et al. 1985; Corselli and Talbot 1987; see Talbot 1985, for review). In addition, cumulus components may stimulate sperm motility (Bradley and Garbers 1983) and induce the acrosome reaction; they may also enhance the fertilizing ability of sperm (Bavister 1982; Tesarik 1985; Meizel and Turner 1986). Recent studies with the hamster (Cherr et al. 1986; Corselli and Talbot 1987) have suggested that capacitated sperm with intact acrosomes or modified acrosomes (Cummins and Yanagimachi 1986) are capable of traversing the entire cumulus matrix. It has been demonstrated that changes in sperm motility occur when non-acrosome reacted hamster sperm enter the matrix (see Katz et al. 1987, for review). Thus, it has been suggested that flagellar motion plays a necessary, if not sufficient role in sperm passage through oocyte investments (Katz et al. 1987). A thorough understanding of the microenvironment that the sperm encounters during gamete interaction requires geometric and physical characterization of the microstructure of the cumulus matrix and zona, in addition to elucidation of their molecular constituents. As in studies of extracellular matrices from other cells, the ultrastructure of the matrix has been observed by transmission electron microscopy (TEM) following staining with cationic dyes (Talbot 1984). While these compounds exhibit a high affinity for acid mucopolysaccharides (Luft 1971) and stabilize the extracellular matrix to some degree, they do not prevent the dramatic shrinkage during preparation (Talbot and DiCarlantonio 1984a). Clearly, preparative techniques that minimize shrinkage of the cumulus and zona would contribute significantly to such work.

In the present study, we have employed freeze substitution to prepare oocyte-cumulus complexes for light- and electron microscopy. This technique has enabled us to view the fine structure of the cumulus matrix and zona for the first time without some of the artifacts that have typically hampered more conventional approaches. More importantly, preparation of samples in this manner has enabled ultrastructural assessment of the impact of the sperm on the cumulus matrix and zona, as well as the effects of these matrices on sperm functions, e.g., the acrosome reaction and movement characteristics.

Materials and methods

Hamsters

Golden hamsters (*Mesocricetus auratus;* 8 weeks old) were obtained from Charles Rivers Labs (Wilmington, Massachusetts) and Simonson Labs (Gilroy, California). All were

Send offprint requests to: Dr. David F. Katz, Department of Obstetrics and Gynecology, School of Medicine, University of California, Davis, CA 95616, USA

Halozyme EX2102
Merck v. Halozyme
PGR2025-00053

held in a 14:10 light:dark cycle. For some animals, the light cycle was reversed such that the dark cycle began at 7 a.m.

Chemicals

All chemicals used in the preparation of media or injections were purchased from Sigma Chemical Company (St. Louis, Missouri). Supplies for electron microscopy were obtained from Ted Pella (Tustin, California).

Media

Dulbecco's phosphate-buffered saline (PBS) was used to wash all gametes. The concentrations of salts were 144 mM NaCl, 3.15 mM KCl, 8.24 mM Na_2HPO_4, 1.48 mM KH_2PO_4, 0.93 mM $CaCl_2$ 2 H_2O and 0.40 mM $MgCl_2$ 6 H_2O. PBS was stored at 4° C. All gamete incubations were carried out in a modified Tyrode's buffer in which the salt concentrations were 123 mM NaCl, 3.1 mM KCl, 0.3 mM NaH_2PO_4 H_2O, 24.9 mM $NaHCO_3$, 2 mM $CaCl_2 \cdot 2\,H_2O$, 0.4 mM $MgCl_2 \cdot 6\,H_2O$. Media for sperm capacitation and fertilization (FM) also contained 0.5 mM taurine, 0.5 mM glucose, 0.25 mM pyruvate, 12.5 mM Na-lactate and 12.5 mg bovine serum albumin (BSA). The pH of this solution was adjusted to 7.3 with CO_2.

Oocyte collection

Mature female hamsters were stimulated to superovulate by an intraperitoneal injection of 25 IU of pregnant mare serum gonadotropin (PMSG), followed by injection of 25 IU of human chorionic gonadotropin (HCG) at least 60 h later. They were sacrificed 12.5 h after the HCG injection. In some experiments, female hamsters were tested for their stage of the estrous cycle so that unstimulated ovaries could be used. The products of naturally stimulated ovulation tended to exhibit less variability.

Female hamsters were monitored for receptivity to males; if receptive, they were removed and sacrificed 4–5 h after the onset of the dark cycle. Excised ovaries were rinsed in PBS (pH 7.2) and dissected to remove peripheral tissue.

Mature follicles were then ruptured, the external granulosa wall removed and the oocyte-cumulus complex was gently teased from the follicle (Talbot 1983). Isolated oocyte-cumulus complexes were thrice rinsed and placed in FM. OCC's were kept at 37° C and after isolation were maintained in an atmosphere of 5% CO_2, 95% air. After 30 min, OCC's were either fixed or incubated with sperm.

Sperm collection

Caudal epididymal sperm were obtained and capacitated according to Meizel and Turner (1983), as modified by Cherr et al. (1986). Only sperm suspensions with >70% motility, of which 70% of the cells exhibited hyperactivated motility after 3.5–4.0 h of incubation, were used in the gamete interaction studies.

Sperm-egg interaction

OCC's (10) pipetted into 500 µl fresh FM were overlaid with paraffin oil (37° C) that had been previously equilibrated in CO_2 and buffer. Sperm suspensions were generally diluted prior to combining with OCC's, such that a final ratio of 20–100 sperm/OCC was achieved. Under these conditions, 6–10 sperm were found within an OCC after 20 min. Following introduction of sperm, samples were coincubated at 37° C under 5% CO_2 and 95% air for either 10 or 20 min prior to fixation.

Processing for electron microscopy

OCC's were prepared for electron microscopy by modifying a previously reported technique for freeze substitution (Murata et al. 1985; see Gilkey and Staehelin 1986, for review). OCC's with and without sperm were prefixed at the appropriate times by adding 100 µl of 2.5% glutaraldehyde-buffered in 0.1 M cacodylate (pH 7.3). After 5–10 min, the OCC's were transferred to fresh 0.1 M cacodylate-buffered 2.5% glutaraldehyde to which 0.25% acrolein had been added. OCC's were fixed for 1 h, and then thoroughly washed in 0.1 M cacodylate overnight. Samples were postfixed in 0.1% tannic acid for 2 h. Thereafter samples were washed for at least 4 h in 0.1 M cacodylate. Washed OCC's were placed in a 10% DMSO −0.1 M cacodylate solution for at least 30 min.

OCC's were then placed in 3-mm gold freeze-fracture caps; excess liquid was removed with filter paper. Gaseous freon-22 was injected into a small well and bathed in liquid nitrogen (LN_2) until it liquified and eventually solidified. A hexagonal wrench was then inserted into the frozen freon to liquefy it. The cap containing the OCC was then immersed for 30 sec and immediately placed in LN_2. This process was continued until all OCC were in LN_2. The caps containing OCC were then transferred to 100% methanol that had been cooled to −70° C with a dry ice bath. They were then placed in a Revco freezer (−80° C). After 72 h the 100% methanol was replaced with 0.1% OsO_4 in 100% methanol, and placed in a freezer at −20° C for 4–8 h. After removal of the H_2O, the sample usually floated free from the gold caps. Samples were brought up to room temperature (1 h), washed twice in 100% methanol, and then placed overnight in a 50:50 mixture of Spurrs' epoxy resin and 100% methanol. The samples were infiltrated with resin for 4 h and then embedded overnight.

Samples were sectioned with glass and diamond knives. The 0.5-µm thick sections were stained according to del Cerro et al. (1980), a procedure that enhanced the appearance of the extracellular matrix. For TEM, sections of the OCC were cut on a diamond knife and stained with uranyl acetate and lead citrate. Observations and photography were performed on a Philips 410 TEM.

Samples used for scanning electron microscopy (SEM) were prepared as previously described and then critical-point dried before sputter coating with gold. Micrographs were taken on a Philips 501 SEM.

Results

Cumulus and zona material

After puncturing a mature follicle, the OCC was immediately expelled. The mature OCC usually continued to expand until it had increased in diameter by approximately 10%. Whether this expansion was due to continued hydration, dilution of follicular fluid or rebounding from elastic compression is not yet clear. However, it should be noted that

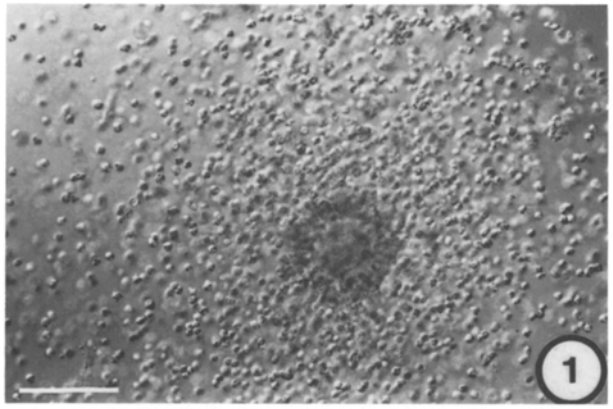

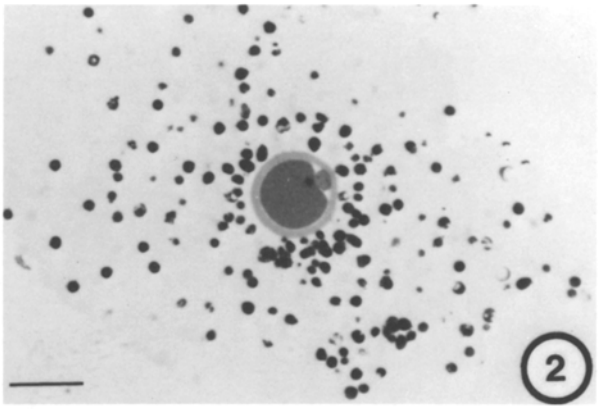

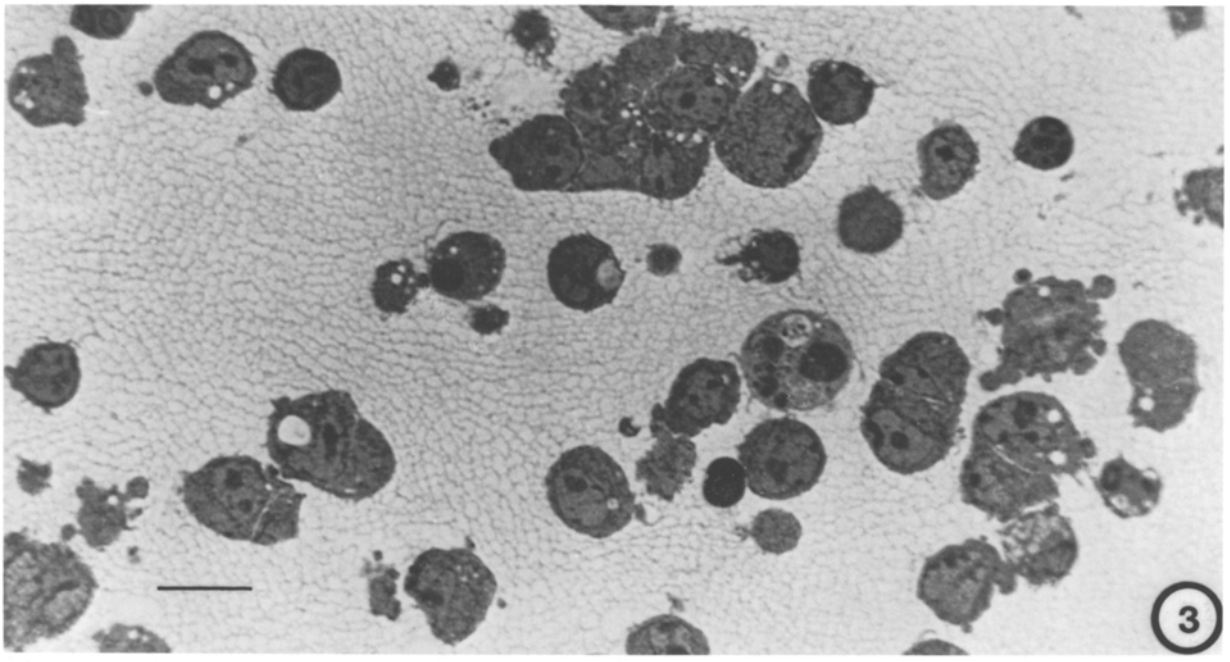

Fig. 1. Nomarski phase-contrast view of an oocyte-cumulus complex (OCC). Bar = 100 μm

Fig. 2. Low magnification of a thick section through an entire oocyte-cumulus complex. Bar = 100 μm

Fig. 3. A higher magnification of a thick section revealing cumulus cells embedded in the extracellular matrix. Bar = 1 μm

all OCC's observed expanded after follicular expulsion. The effective diameter of a complex was typically between 0.75–0.85 mm. None of the samples prepared for TEM exhibited any overall reduction in diameter greater than 5%. In general, structural features of the ovulated and follicular cumulus matrix were similar. Therefore, all the micrographs presented here are of follicular material.

Follicular complexes were nearly spherical, with the oocyte usually centrally positioned (Fig. 1). The cumulus matrix was translucent, with numerous cells distributed throughout. The local density of cumulus cells appeared to decrease with distance from the oocyte. The innermost layers of cells are referred to as the corona radiata. This layer could be distinguished in follicular complexes, but was less conspicuous in oviducal complexes. Another morphological feature unique to follicular complexes was the presence of large aggregates of cumulus cells, sometimes up to ten cells within a cluster (Figs. 2, 3). Although clusters were seen in the ovulated cumulus masses, the cells within a cluster usually numbered less than three. A section through the cumulus matrix revealed a uniform fibrous network among cells (Fig. 3). The matrix appeared continuous with no obvious cavities or "channels" (Fig. 3). The external surface of the complex also appeared to be continuous.

The underlying matrix had an extensive network of fibrillar material that was, for the most part, uniformly distributed (Fig. 4). The matrix material was closely apposed to the cumulus cells (Fig. 5). The fibrillar elements appeared to have attachment sites on the cells, such sites being associated with cell filopodia (Fig. 6). Cumulus cells were usually spherical, with large, centrally positioned nuclei. Abundant mitochondria and arrays of smooth endoplasmic reticulum were also present (Fig. 5). The cumulus matrix appeared to run parallel to the cell membrane, while individual fibrillar elements branched down to the filopodial extensions (Fig. 6). There were no regions within the lattice-like microstructure with preferred orientation of fibrils, i.e., there was no obvious sign of "cords" in the material. The

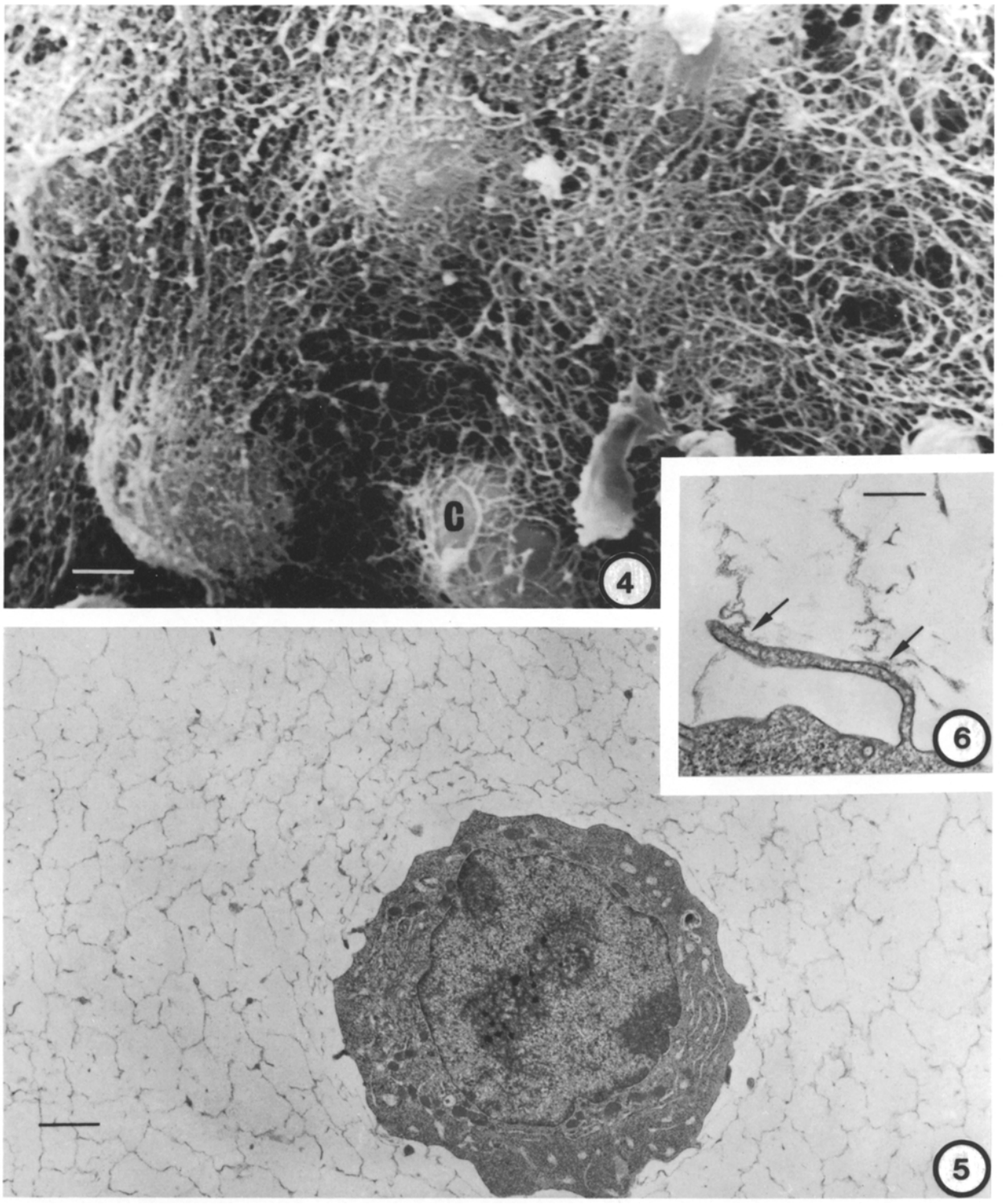

Fig. 4. Inner cumulus matrix as viewed with SEM showing a highly branched filamentous substructure. Cumulus cells (*C*) can also be observed. Bar = 2.8 μm

Fig. 5. A cumulus cell embedded in the extracellular matrix. Bar = 1.3 μm

Fig. 6. Filopodial extensions (*arrows*) are typically sites where the extracellular matrix appears to attach to cumulus cells. Bar = 0.36 μm

interstitial or "pore" diameter between the fibrillar elements varied, but was usually between 0.5–0.8 μm. Individual fibrils were approximately 50–100 nm in diameter. They appeared to have a cylindrical to ribbon-like configuration which was twisted or coiled, giving it an alternating thick-thin appearance (Figs. 5, 6). The junctions at which the fibrils connect were always structured as "Y joints". There was some thickening of material at these junctions, but they did not appear, morphologically, to be specialized. Although the visually darker fibrillar elements were the

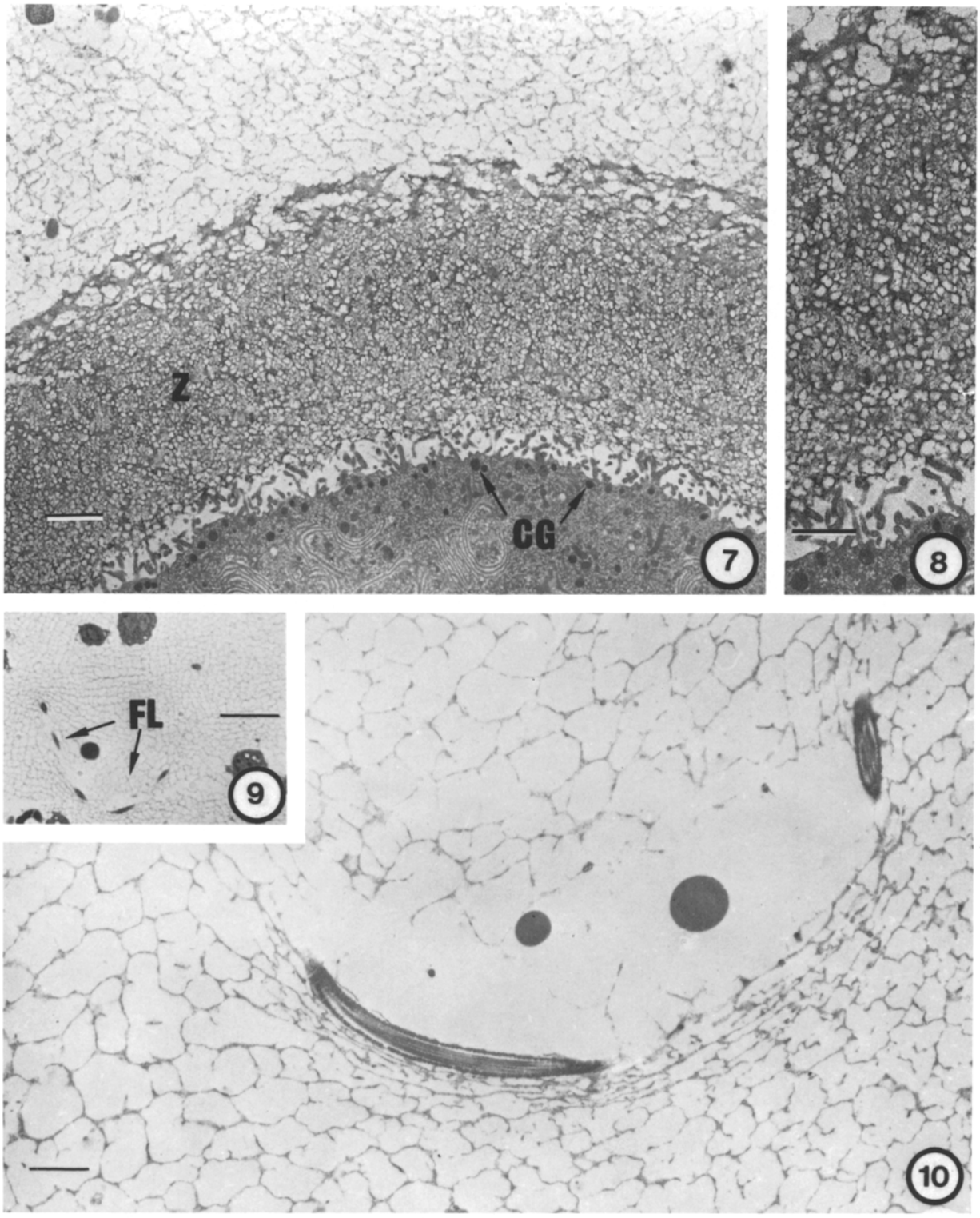

Fig. 7. Extracellular matrix, zona pellucida (*Z*) and oocyte. The matrix penetrates the outer crypts of the zona. Also note the porous nature of the zona and the presence of cortical granules (*CG*) at periphery of oocyte. Bar = 1.6 μm

Fig. 8. Higher magnification of zona pellucida. Bar = 2.7 μm

Fig. 9. Longitudinal section through the flagellum (*FL*) within the cumulus matrix. Bar = 3 μm

Fig. 10. Fine-structural view of the flagellum-matrix interaction. Note the tear and compaction of the matrix on either side of the flagellum. Bar = 1.1 μm

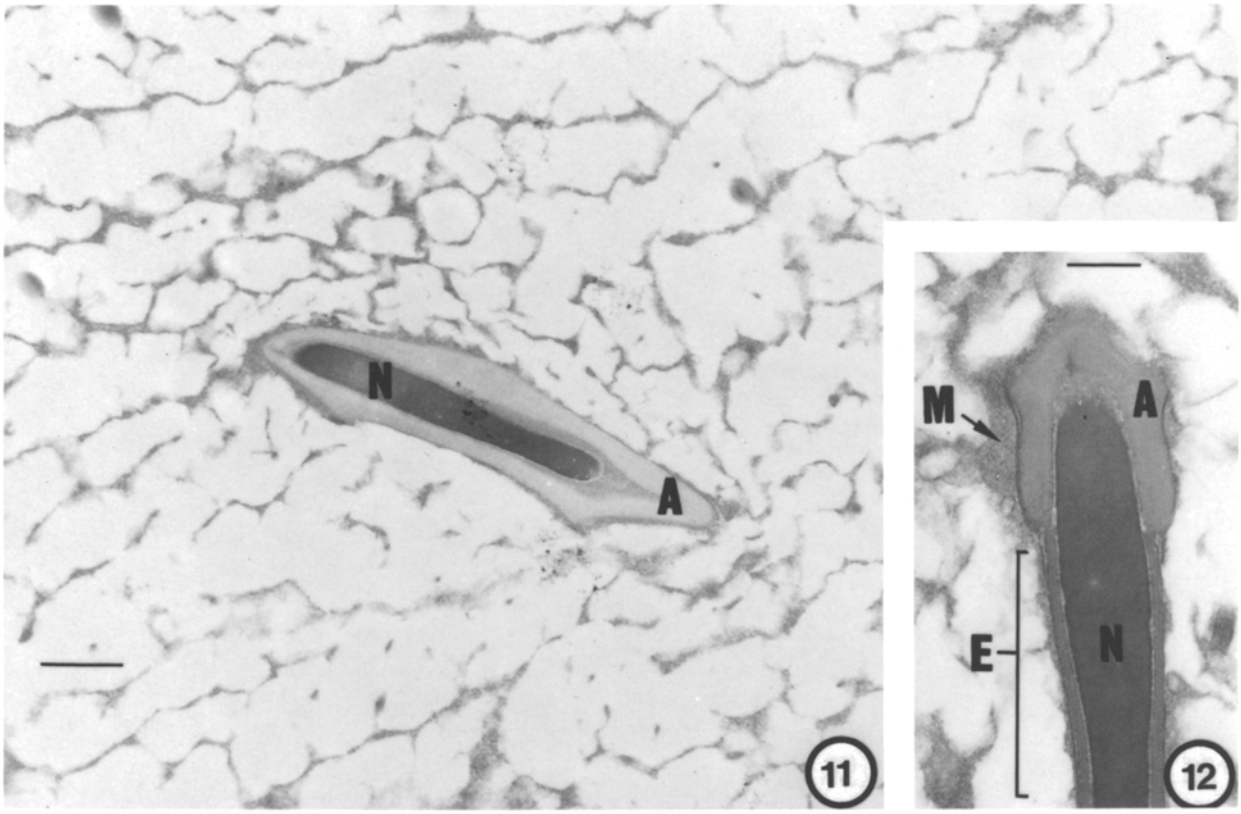

Fig. 11. Section through head region of a sperm within the matrix. The matrix appears to be slightly compressed and in close apposition to the concave surface of the sperm head. Note the nucleus (*N*) and intact acrosome (*A*). Bar = 0.7 μm

Fig. 12. Higher magnification showing the matrix (*M*) intimately in contact with sperm surface. The acrosome (*A*) of this sperm also appears morphologically intact. Nucleus (*N*), equatorial segment (*E*). Bar = 0.3 μm

most prominent, higher magnification reveals an intrapore substructure (Fig. 6) in which the elements are also fibrillar but are much thinner. These intrapore elements never ran continuously from one major fibrillar element to another. Such an appearance could be real, or simply reflect disruption of the smaller filaments because of their fragile nature. Overall, the appearance of the fibrillar network changed little from the outer margin of the cumulus to the zona pellucida, although slight morphological differences were evident within the corona radiata layer.

Cumulus cells were seldom found in close association with the zona pellucida. The matrix material extended into large crevices on the margin of the zona (Fig. 7). These pores ranged in size from 80 nm to 160 nm diameter. This outer edge had a pronounced "jagged" appearance. Overall, the zona had a marked uniform porous nature (Figs. 7, 8). The microvilli from the oocyte extended through the perivitelline space and often contacted the zona (Fig. 8). There was no obvious appearance of particulate material within the perivitelline space. Cortical granules could be observed at the periphery of the oocyte, and the oocyte cytoplasm appeared similar to that seen with other techniques of fixation.

Sperm within the cumulus matrix

The lateral motions of the flagellum appeared to compress the local matrix microstructure in front of its advancing surface; behind that surface the microstructure was characteristically stretched, or even torn in some instances (Figs. 9, 10). Such tearing of the microstructure in the interior of the matrix was usually observed in such regions "behind" the bending flagellum. In general, the microstructure appeared to rebound to its original configuration after sperm passage. It is interesting that in the longitudinally sectioned flagellum, there were periodically spaced regions in and out of the plane of section (Figs. 9, 10). This implies a three-dimensional component to flagellar bending, with a different periodicity (7–10 μm) from that in the principal plane of bending.

Only slight compression of the cumulus matrix adjacent to the sperm head was observed (Fig. 11). The lack of apparent distortion of microstructure adjacent to the sperm head was probably because the velocity vector of the head was not generally in the plane of section. The matrix microstructure did not show any sign of degradation adjacent to the sperm head. Indeed, the matrix was intimately associated with the plasma membrane (Figs. 11, 12). In seven cases in which sperm heads were sectioned, the matrix microstructure was always in close contact with the head surface, often with fibrils aligned along the plasma membrane. All of these sperm, which were distributed throughout the cumulus, had morphologically intact acrosomes. No sperm were observed in the corona radiata layer. There was no evidence of acrosomal swelling, decondensation of acrosomal matrix, or vesiculation.

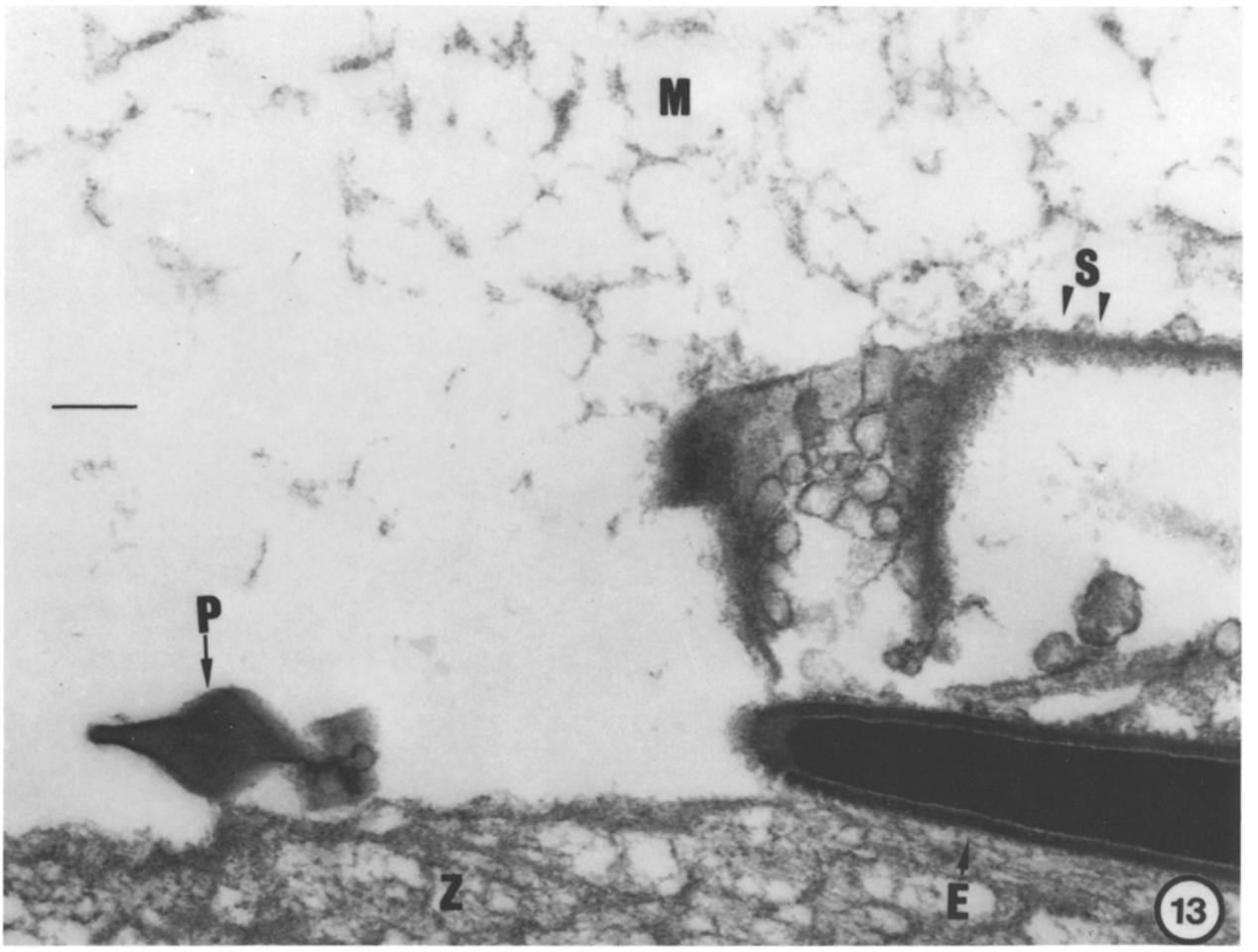

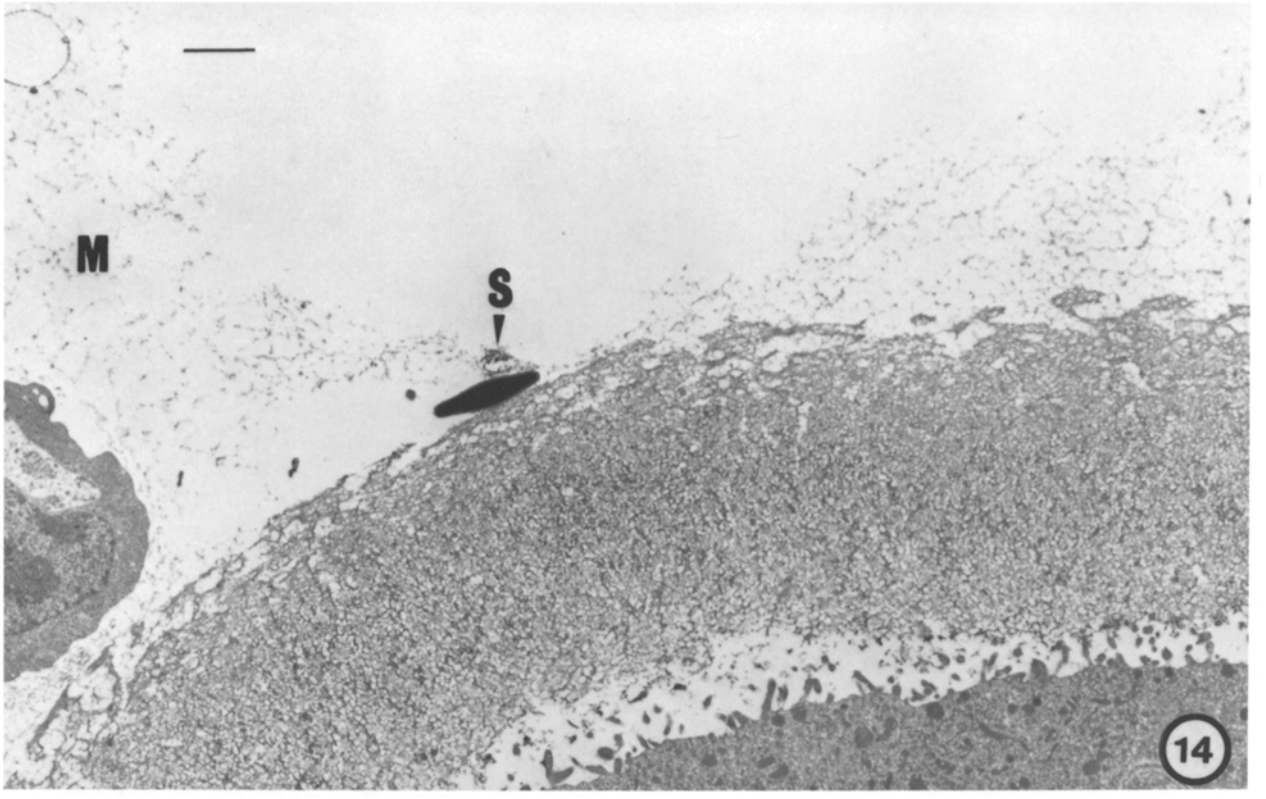

Fig. 13. A sperm undergoing an acrosome reaction on the zona (*Z*). The vesiculated shroud (*S*) has lifted off as the sperm moves through it; the perforitorium is now the leading edge. Note the compression of the zona under the equatorial segment (*E*). Cumulus matrix (*M*) is still present although it has lost some of its structural integrity. Bar = 0.25 μm

Fig. 14. Section through the head of an acrosome-reacted sperm on the zona. Remnants of the shroud (*S*) are still present but the matrix (*M*) has been morphologically altered or is completely absent in close proximity to the head. Bar = 1.75 μm

Sperm on the zona pellucida

Four spermatozoa were sectioned while in contact with the outer surface of the zona, but not penetrating it. All had initiated or completed the acrosome reaction. Here, the adjacent cumulus microstructure had undergone dramatic morphological changes (Fig. 13). In other localized regions, the fibrillar network was present but changed: there were no longer any interconnections between individual fibrils, and the length of these fibrils was diminished (Fig. 13). The appearance was, thus, one of a fragmented network. When the acrosomal shroud, i.e., remnants of the plasma and outer-acrosomal membranes was present, the fragmented fibrils were in contact with it. Zonae adjacent to sperm exhibited a degree of local compression, but no obvious sign of digestion (Fig. 13). In some instances the matrix was absent in a localized region around the sperm (Fig. 14). Here, no matrix extended into the jagged external pores of the zona (Fig. 14).

Discussion

It has been reported that a major macromolecular component of the cumulus matrix is hyaluronic acid (Ball et al. 1982), and that it may in fact be structured in the form of a glycosaminoglycan (GAG) involving chondroitin sulfate and core proteins, as has been described in studies of other extracellular matrices (Hascall 1980). The GAG nature of the cumulus matrix would thus lend integrity to its microstructure, the chondroitin sulfate-protein monomers serving as links between the hyaluronic acid structure (Faltz et al. 1979). Hyaluronic acid is known to exist in at least four different configurations. One of these has a reduced axial periodicity, which creates a secondary structure that is relatively stiff compared to other GAG's (see Arnott and Mitra 1984 for review). Much of our knowledge of GAG's, and extracellular matrices in general has been derived from other systems. Thus, there remains a need for better understanding of the molecular composition and configuration of the cumulus matrix.

Historically, visualization of the extracellular matrix has been difficult due to the hydrated nature of GAG's. For example, SEM or TEM with cationic dyes have been employed to discern the structure of the extracellular matrix of the cumulus (Phillips and Dekel 1982; Talbot 1984; Talbot and DiCarlantonio 1984b). These studies have been insightful, but they involve some degree of artifact due to the large amount of shrinkage in the cumulus material (Talbot and DiCarlantonio 1984a). Our modified technique of freeze substitution has resulted in remarkably good preservation of both the oocyte and cumulus cells as well as the cumulus matrix. It is not surprising, therefore, that our "view" of the cumulus matrix, and indeed of the zona pellucida, differs somewhat from those previously described. We have found that the cumulus-matrix microstructure in the golden hamster consists of a network of fibrillar units with a considerable amount of interconnection. For the most part, the matrix appeared as a homogenous, fibrillar network throughout the OCC, although subtle differences in the corona radiata associated matrix were observed. The interstitial pores are less than the diameter of the sperm head. We saw no evidence of any channels or "paths of least resistance" in the microstructure prior to its interaction with sperm.

Because this perception of the cumulus matrix indicates that penetrating sperm are in very intimate association with its microstructure, strong biomechanical and molecular interactions can be expected to occur. Indeed, our micrographs illustrate local deformation of the matrix microstructure adjacent to the moving flagellum and sperm head. Such deformation is suggestive of increased local resistance to flagellar movement, in that individual fibrils appeared bent and/or stretched and local pores were compressed and/or stretched. These findings are entirely consistent with observations of hamster sperm motility within the cumulus (Cummins and Yanagimachi 1982; Suarez et al. 1984; Drobnis et al. 1986; Katz et al. 1986, 1987; Corselli and Talbot 1986). In these studies the flagella of such spermatozoa were seen to bend with conspicuously less curvature than when in the low viscosity fluid surrounding the cumulus, with the implication that the flagellum must push considerably harder per unit velocity (viscosity) and/or per unit displacement (elasticity). It is interesting that our micrographs revealed a periodic three-dimensional component to flagellar bending, with wavelength considerably shorter than that of the principal bends. To our knowledge, this form of three-dimensionality has not previously been reported for mammalian spermatozoa. Whether it is a unique consequence of the sperm-cumulus interaction, or a more ubiquitous property of mammalian sperm flagellar bending, is not yet known.

The quantitative and qualitative nature of the local cumulus resistance to sperm is not yet understood. However, the present observations, combined with more detailed measurements of sperm movement characteristics during cumulus penetration (E. Drobnis, pers. comm.) offer some new insights. During penetration, the sperm head deforms and may even tear the local microstructure adjacent to it. Our micrographs of sperm heads within the cumulus revealed bending and stretching of the adjacent microstructure but little obvious tearing. This does not imply that no such tearing exists; to visualize the maximum degree of matrix distortion, the plane of the thin-microscopic section must contain the instantaneous axis of sperm head translation. Indeed, our micrographs of flagella in the cumulus did reveal adjacent regions devoid of microstructure. These two-dimensional cavities could reflect a three-dimensional tubular "wake" sheared by the advancing sperm head, the flagellum following the head along the path of least resistance. "Snakelike" motions of sperm in the cumulus have been observed, the flagellum following in the exact path of the head while effectively propagating waves of large amplitude but very low frequency (Suarez et al. 1983, 1984; E. Drobnis, pers. comm.). Such trajectories would, thus, effect a local clearing/alteration of matrix material along a narrow, serpentine path. Preliminary mathematical analysis of the hydrodynamics of sperm movement in viscoelastic materials indicates that such serpentine movement reflects a strong elastic component in the cumulus resistance to sperm (Katz, unpublished).

It is possible that sperm enzymes, e.g., hyaluronidase, could also contribute to a reduction in local cumulus resistance to sperm motion. Mammalian spermatozoa contain this enzyme both on the surface of the plasma membrane and within the acrosome (Zao et al. 1985). While the majority of surface hyaluronidase is released prior to capacitation (Zao et al. 1985), it is possible that some may be available to contribute to cumulus penetration prior to the occur-

rence of the acrosome reaction. We often saw fibrils of the microstructure aligned parallel to and virtually in contact with the sperm plasma membrane. Thus, if sperm surface hyaluronidase were acting upon the cumulus matrix in our preparations, it must have done so in an extremely localized and/or limited fashion.

Previous light-microscopic studies have documented that capacitated, non-acrosome-reacted hamster sperm can routinely traverse the entire cumulus matrix and bind to the zona, at which point they then complete the acrosome reaction (Suarez et al. 1984; Bavister 1985; Corselli and Talbot 1986; Cherr et al. 1986; Katz et al. 1986). In our experiments, spermatozoa in the cumulus matrix were acrosome-intact; only sperm associated with the zona initiated the acrosome reaction. Moreover, we saw no ultrastructural evidence of early phases of the acrosome reaction in spermatozoa distributed throughout the cumulus matrix, as has been suggested by Cummins and Yanagimachi (1986).

We observed a very different picture of the cumulus microstructure adjacent to those spermatozoa in contact with the zona surface. Locally, the fibrils here were often shorter with fewer interconnections; or the microstructure was absent altogether, giving rise to cavities adjacent to the sperm. In principle, two factors could have contributed to this appearance: enzymatic activity and/or sustained mechanical action of the sperm flagellum. We cannot as yet be certain of the relative importance of these two factors here, since sustained oscillatory shearing (as by the flagellum) can degrade many biopolymers and perhaps the cumulus matrix. Indeed, we do not yet appreciate the functional significance of these cleared or altered regions. They could contribute in some way to proper sperm orientation and/or thrust against the zona; or they could simply be an epiphenomenon indicative, perhaps, of the occurrence of the acrosome reaction. Talbot (1984) demonstrated that cumulus matrix components were present in the pores of the hamster zona pellucida and suggested that hyaluronidase, released during the acrosome reaction, might facilitate sperm penetration of the zona. Our results are relevant to this hypothesis. There was no matrix material in the peripheral zona pores close to bound acrosome-reacted sperm, a consequence, perhaps, of hyaluronidase activity.

Earlier investigators of the permeability of the zona pellucida speculated that it was impermeable to molecules with molecular weight greater than 16000 (Austin and Lovelock 1958). However, this was later refuted by Enders (1971), who demonstrated that ferritin particles (11 nm) and even much larger thorotrast molecules could easily diffuse across the rat zona pellucida. Gwatkin (1966) found that virus particles (28 nm) could infect mouse oocytes with intact zonae. Thus, it was proposed that the zona pellucida is highly porous, and thereby allows the exchange of soluble and possibly insoluble molecules. This view of the zona was not presented in previous fine structural studies, which depicted its inner region as relatively compact. In contrast, our work has revealed a highly porous structure throughout the zona, a view that is consistent with the earlier studies of molecular transport across the zona.

The fixation technique used in this study has given us new insight into the basic structure of extracellular matrices, and has also provided a "sperm's-eye view" of the oocyte investments. Such observations, coupled with real-time analyses of sperm penetration of the cumulus and zona pellucida, should contribute to a more thorough understanding of sperm-egg investment interactions.

Acknowledgments. We appreciate the words of wisdom and constant encouragement from Ms. Greta Fry and Mr. Robert Munn. We extend our thanks to Dr. Wallis H. Clark, Jr. for the use of laboratory equipment, Drs. Carol Erickson and Prudence Talbot for their helpful suggestions, and to Beth Clark, who made long-distance preparation of the manuscript a reality. This work was supported by NIH grant HD 12971.

References

Arnott S, Mitra AK (1984) X-Ray diffraction analysis of glycosaminoglycans. In: Arnott S, Rees DA, Morris ER, (eds) Molecular biophysics of the extracellular matrix. Humana Press, Clifton, New Jersey, pp 41–67

Austin CR, Lovelock JE (1958) Permeability of rabbit, rat and hamster egg membranes. Exp Cell Res 15:260–265

Ball GD, Bellin ME, Ax RL, First NL (1982) Glycosaminoglycans in bovine cumulus-oocyte complexes: Morphology and chemistry. Mol Cell Endocrinol 28:113–122

Bavister B (1982) Evidence for a role of post-ovulatory cumulus components in supporting fertilizing ability of hamster spermatozoa. J Androl 3:365–372

Bavister B (1986) Animal in vitro fertilization and embryo development. In: Gwatkin RBL (ed) Manipulation of mammalian development. Plenum Press, New York, pp 81–148

Bradley MP, Garbers DL (1983) The stimulation of bovine caudal epididymal sperm forward motility by bovine cumulus egg complexes in vitro. Biochem Biophys Res Commun 115:777–787

Cerro M del, Cogen J, Cerro C del (1980) Stevenel's Blue, an excellent stain for optical microscopical study of plastic embedded tissues. Microsc ACTA 83(2):117–121

Cherr GN, Lambert H, Meizel S, Katz DF (1986) In vitro studies of the golden hamster acrosome reaction: Completion on the zona pellucida and induction by homologous soluble zonae pellucidae. Dev Biol 114:119–131

Corselli J, Talbot P (1986) An in vitro technique to study penetration of hamster oocyte-cumulus complexes by using physiological numbers of sperm. Gamete Res 13:293–308

Corselli J, Talbot P (1987) In vitro penetration of hamster oocyte-cumulus complexes using physiological numbers of sperm. Dev Biol 122:227–242

Cummins JM, Yanagimachi R (1982) Sperm-egg ratios and the site of the acrosome reaction during in vivo fertilization in the hamster. Gamete Res 5:239–256

Cummins JM, Yanagimachi R (1986) Development of ability to penetrate the cumulus oophorus by hamster spermatozoa capacitated in vitro, in relation to the timing of the acrosome reaction. Gamete Res 15:187–212

Drobnis E, Yudin AI, Katz DF (1986) Kinetic analysis of sperm penetrating the zonae pellucidae of cumulus-intact hamster eggs. J Cell Biol 103 (5, pt. 2):241a

Dunbar BS, Wolgemuth DJ (1984) Structure and function of the mammalian zona pellucida, a unique extracellular matrix. Mod Cell Biol 3:77–111

Enders AC (1971) The fine structure of the blastocyst. In: Blandau RJ (ed) The Biology of the Blastocyst. University of Chicago Press, Chicago, Ill, pp 71–94

Faltz LL, Reddi AH, Hascall GK, Martin D, Pita JC, Hascall VC (1979) Characteristics of proteoglycans extracted from swarm rat chondrosarcoma with associative solvents. J Biol Chem 254:1375–1380

Gilkey JC, Stachelin A (1986) Advances in ultrarapid freezing for the preservation of cellular ultrastructure. J Electron Microsc Tech 3:177–210

Gwatkin RBL (1966) Effect of viruses on early mammalian development. III. Further studies concerning the interaction of Mengo encephalitis virus with mouse ova. Fertil Steril 17:411–418

Hascall GK (1980) Cartilage proteoglycans: Comparison of sectioned and spread whole molecules. J Ultrastruct Res 70:369–375

Katz DF, Cherr GN, Lambert H (1986) The evolution of hamster sperm motility during capacitation and interaction with the ovum vestments in vitro. Gamete Res 14:333–346

Katz DF, Drobnis EZ, Baltz J, Cherr GN, Yudin AI, Cone RA, Cheng LY (1987) The biophysics of sperm penetration of the cumulus and zona pellucida. In: New Horizons in Sperm Cell Research. Japan Scientific Societies Press (In press)

Luft JH (1971) Ruthenium red and violet. II. Fine structural localization in animal tissue. Anat Rec 171:369–416

Meizel S, Turner KO (1983) Seritonin or its agonist 5-methoxytryptamine can stimulate hamster sperm acrosome reactions in a more direct manner that catecholamines. J Exp Zool 226:171–174

Meizel S, Turner KO (1986) Glycosaminoglycans stimulate the acrosome reaction of previously capacitated hamster sperm. J Exp Zool 237:137–139

Murata F, Suzuki S, Tsuyama S, Suganuma T, Imada M, Furihata C (1985) Application of rapid freezing followed by freeze-substitution acrolein fixation for cytochemical studies of the rat stomach. Histochem J 17:967–980

Phillips DM, Dekel N (1982) Effect of gonadotropins and prostaglandin on cumulus mucification in cultures of intact follicles. J Exp Zool 221:275–282

Suarez S, Katz DF, Overstreet JW (1983) Movement characteristics and acrosomal status of rabbit spermatozoa recovered at the site and time of fertilization. Biol Reprod 29:1277–1287

Suarez S, Katz DF, Meizel S (1984) Changes in motility that accompany the acrosome reaction in hyperactivated hamster spermatozoa. Gamete Res 10:253–266

Talbot P (1983) Videotape analysis of hamster ovulation in vitro. J Exp Zool 225:141–148

Talbot P (1984) Hyaluronidase dissolves a component of the hamster zona pellucida. J Exp Zool 229:309–316

Talbot P (1985) Sperm penetration through oocyte investment in mammals. Am J Anat 174:331–346

Talbot P, DiCarlantonio G (1984a) The architecture of the hamster oocyte-cumulus complex. Gamete Res 9:261–272

Talbot P, DiCarlantonio G (1984b) The oocyte-cumulus complex: Ultrastructure of the extracellular matrix in hamster and mice. Gamete Res 10:127–142

Tesarik J (1985) Comparison of acrosome reaction-inducing activities of human cumulus oophorus, follicular fluid and ionophore A23187 in human sperm population of proven fertilizing ability in vitro. J Reprod Fertil 74:383–388

Zao P, Meizel S, Talbot P (1985) Release of hyaluronidase and BN-acetyl hexosaminidase during in vitro incubation of hamster sperm. J Exp Zool 234:63–74

Accepted August 28, 1987